# Hot Compression Deformation Behavior of AE42 Magnesium Alloy

Rui ZHANG[1,a], Bin-Bin TANG[1,b,*], Pei-Peng JIN[1,c]

[1]Qinghai provincial Key Laboratory of New Light Alloys, Qinghai University, Xining 810016,PR China

[a]zruiliu@163.com, [b]tangbb@hotmail.com, [c]jingpeipeng@hotmail.com

*Corresponding author

**Keywords:** AE42 Magnesium Alloy, Hot Compression Deformation, Constitutive Equation, Flow Stress.

**Abstract.** The hot compression deformation behavior of AE42 magnesium alloy was investigated at the temperature range from 250 to 450 ℃, the strain rate range from 0.001 to10 $s^{-1}$ and the maximum reduction of 60 %. The relationships between flow stresses, deformation temperatures and strain rates of AE42 magnesium alloy were analyzed. The constitutive equation at elevated temperature was given. The results show that the flow stress decreases with the increasing of deformation temperature and the decreasing of strain rate, which can be described by a constitutive equation in hyperbolic sine law as $\dot{\varepsilon}=A[\sinh(\alpha\sigma)]^n\exp(-Q/RT)$, and can also be described by Zener-Hollomon parameters, calculated A, α, n and Q are $4.64\times10^{12}$ $s^{-1}$, 0.0151 $MPa^{-1}$, 7.34 and 173.29 kJ/mol, respectively. The dominated soften mechanisms of the AE42 magnesium alloy transform from dynamic recovery to dynamic recrystallization with increasing of the temperature and decreasing of the strain rate.

## Introduction

Magnesium and its alloys have been attractive for components in various automobile and aerospace applications due to its light density, high specific strength [1]. The consumption of a large amount of magnesium alloys in the automobile industries is an effective strategy for improving fuel efficiency of vehicles [2]. In the passed two decades, AE magnesium alloys are developed by Dow Chemical Company of USA which contain the aluminum and rare earth elements [3], they have high tensile strength at both room temperature and elevated temperature, better creep resistance (more than 200 ℃) than commercially available magnesium alloys (e.g. AZ91 alloy) and corrosion resistance. They have been used in gearbox [4-7]. However, the major limitation for the application of magnesium alloy is its poor formability at or near room temperature due to magnesium only has two independent basal slip systems. The ideal hot workability of the AE alloys is an important reason for the extensive application of the AE magnesium alloys. Therefore, Therefore, it is very important to understand magnesium alloys behavior at hot compression condition for the researchers of metal forming processes (hot extrusion, forging and rolling) which non-basal slip systems could be activated.

Although a large amount of investigation invested into the hot compression behavior of magnesium alloys, there is little research focusing on the behavior of AE42 magnesium alloy. The aim of present work is to investigate the hot compression deformation behavior, analyze the flow stress behavior in terms of strain rate and deformation temperature sensitivities and calculate constitutive equation of AE42 magnesium alloys.

## Experimental procedures

The composition of AE42 (wt%) is shown in Table.1. The ingots of the AE42 alloy were machined to cylindrical specimens with 10 mm in diameter and 15 mm in height. The specimens were homogenized for 12 h at a temperature of 400 ℃. Hot compression tests were performed on a Gleeble-3500 thermal simulation machine at temperatures of 250, 300, 350, 400 and 450 ℃ and the strain rates of 0.001, 0.01, 0.1,1 and 10 $s^{-1}$, respectively. And the heating rate is5 ℃/s. Before the compression tests, the specimens were held at testing temperature for 60 s to achieve uniform temperature throughout the specimens. It ensures the uniform temperature in the specimens Graphite

 

lubricant was used to reduce friction between the die and specimen. The specimens were deformed up to a true stain of ~0.6, and quenched in water immediately after hot compression.

The deformed OM samples were sectioned parallel to the compression axis along the direction of centerline and polished according to the standard metallographic specimen preparation procedure and as-cast OM samples is etched with 8% nitric acid-ethyl alcohol reagent. The microstructure of the alloy was observed by optical microscope (OM, LEICA DMI 3000M).

Tab. 1 Chemical composition of AE42 Mg alloy (wt %)

| Element | Al | Si | Ce | La | Mn | Zn | Mg |
|---|---|---|---|---|---|---|---|
| Fraction | 4.38 | 0.023 | 1.59 | 0.36 | 0.33 | 0.039 | Bal |

## Result and Discussion

### The OM Microstructures and True Stress-stain Curves

The initial microstructures of as-cast and as-homogenized AE42 Mg alloys are shown in Fig.1. The as-cast alloy exhibited a typical cast microstructure. It is consist of α -Mg and Al11Re3 phases at the grain boundaries as shown in Fig.1 (a). It can be see that the second phase does not disappear but more homogenize after the homogenization heat treatment than that of as-cast state.

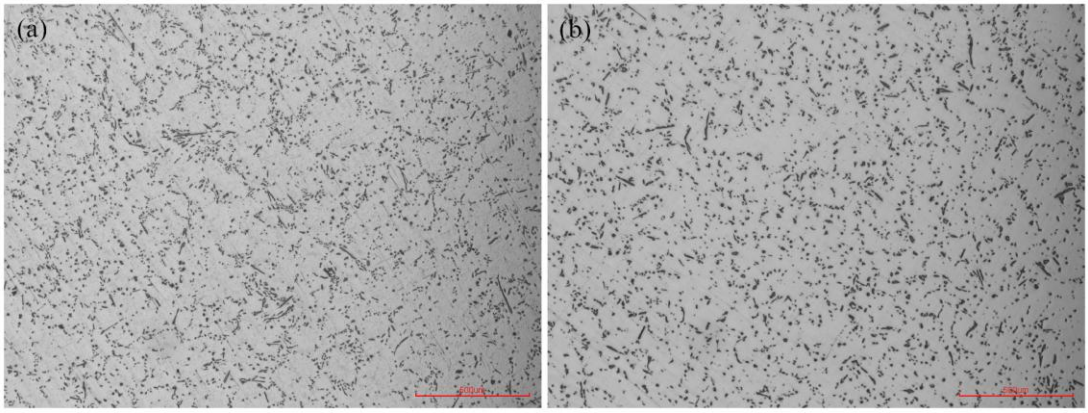


Fig.1 Optical images of the microstructures of the AE42 magnesium alloy: (a) as-cast and (b) as-homogenized

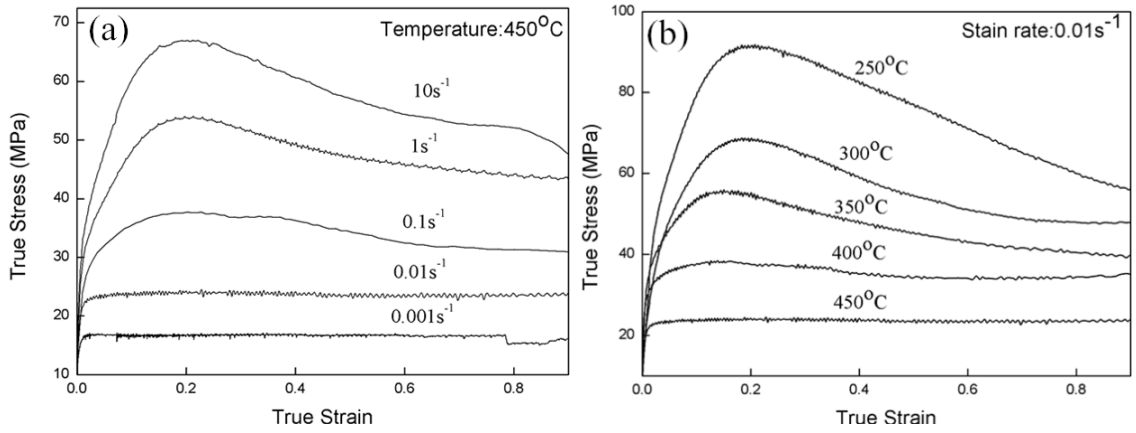


Fig.2 True stress-stain curves of AE42 magnesium alloy under different temperature and stain rate: (a)stain rate 0.01 s-1 and (b)temperature 450 ℃

Because true stress-strain curves at varied conditions have similar trend, therefore the true stress-strain curves at the temperature of 450 ℃and at stain rates of 0.01 $s^{-1}$ was chosen to discuss the phenomena and forming mechanisms of the AE42 in these curves as shown in Fig.2. The flow stress

increases sharply with increasing strain in the initial stage of the deformation process due to working hardening caused by dislocation pile-up, reduplication, and tangle [8], until it reaches a peak stress where dynamic softening occurs caused by the dislocation rearrangement and the counteraction of dislocations [9], and the flow stress tends to become steady owing to the dynamic balance between working hardening and softening. The softening is attributed to the dynamic recovery (DRV) and the dynamic recrystallization (DRX) [10]. The flow curves exhibit typical flow behavior with the interaction of working hardening and dynamic softening. The effects of temperature and stain rate on flow stress are dominant parameters for all experimental conditions. The flow stress decreases with temperature increasing and stain rate decreasing. The rates of hardening and softening with stain vary according to deformation temperature and stain rate. The effect of work hardening is more noticeable at low temperature and/or high stain rate [11]. On the other hand, a dynamic equilibrium between hardening and softening occurs at very initial stage of deformation at high temperature and/or low stain rate [12].

**Constitutive Equation of Flow Stress**

The power law (Eq.1), the exponential law (Eq.2), and the hyperbolic sine law (Eq.3) have been applied for description of the relationship between the strain rate and flow stress [13] in this paper. It is found that the relationship between stress and stain rate in low stress level can be described as follows [14]:

$$\dot{\varepsilon} = A^{'}\sigma^{n^{'}} \exp(-\frac{Q}{RT}) \tag{1}$$

Where $A'$ and $n'$ are the material constants; $\dot{\varepsilon}$ is the stain rate; σ is the flow stress; R is the mole gas constant with the value of 8.314 J/(K • mol-1); $T$ is the temperature; $Q$ is the deformation activity energy which is the critical parameter and reflects the difficult degree of hot deformation process. In the high stress level, the constitutive law can be expressed as in [15]:

$$\dot{\varepsilon} = A^{''}\exp(\beta\sigma)\exp(-\frac{Q}{RT}) \tag{2}$$

Where $A''$ and $\beta$ are also the material constants.

The Arrhenius relationship [16] is suitable for over a wide range of temperature and strain rate.

$$\dot{\varepsilon} = A(\sinh(\alpha\sigma))^n \exp(-\frac{Q}{RT}) \tag{3}$$

Where the stain stress exponent n can be expressed by the stain rate sensitivity $m$ ($n$=1/$m$); and $n$=$\beta$/$\alpha$.

To simplify the equations, get the natural logarithms of both sides for Eq.1-3. Then we have:

$$\ln\dot{\varepsilon} = \ln A^{'} + n^{'}\ln\sigma - \frac{Q}{RT} \tag{4}$$

$$\ln\dot{\varepsilon} = \ln A^{''} + \beta\sigma - \frac{Q}{RT} \tag{5}$$

$$\ln\dot{\varepsilon} = \ln A + n\ln(\sinh(\alpha\sigma)) - \frac{Q}{RT} \tag{6}$$

Based on Eq. 4 and Eq. 5, $\ln\dot{\varepsilon}$ vs. lnσ and $\ln\dot{\varepsilon}$ vs. σ curves were plotted in Fig. 3 and Fig. 4, and the slope of curves were used for obtaining the values of $n'$ and $\beta$, respectively. The values of $n'$ and $\beta$ can

be obtained for different deformation temperatures by liner fitting method, and the mean values of $n'$ and $\beta$ can be calculated as 11.4325 $MPa^{-1}$ and 0.1727 $MPa^{-1}$, respectively.

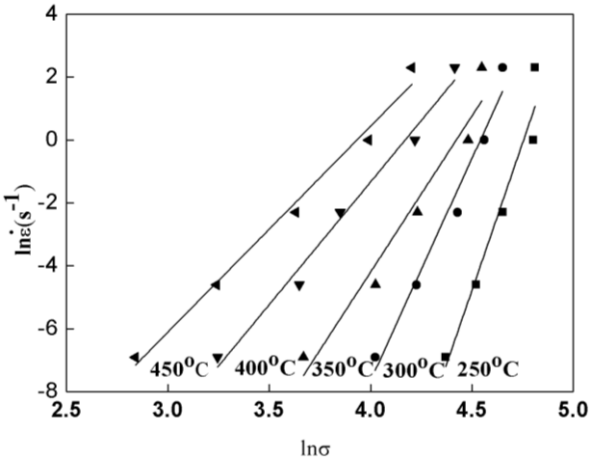


Fig. 3 Relationship between lnσ-$\ln\dot{\varepsilon}$

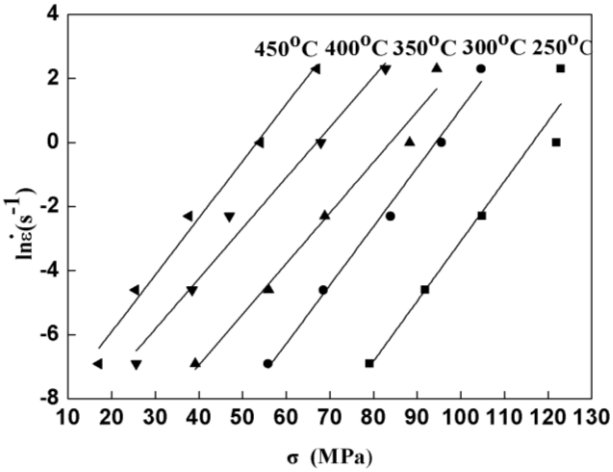


Fig. 4 Relationship between σ-$\ln\dot{\varepsilon}$

The hot compression activation energy $Q$ serving as indicator of deformation difficulty degree in plasticity deformation and can be calculated by the following equation [17]:

$$Q = R\left(\frac{\partial \ln(\sinh(\alpha\sigma))}{\partial(1/T)}\right)_{\dot{\varepsilon}}\left(\frac{\partial \ln\dot{\varepsilon}}{\partial \ln(\sinh(\alpha\sigma))}\right)_{T} \tag{7}$$

From Eq. 6 and 7, the slopes of $\ln\dot{\varepsilon}$ vs. ln[sinh(ασ)] curves can be used for obtaining the value of n shown in Fig. 5, and the slopes of sinh(ln(ασ)) vs. 1000/T is shown in Fig. 6. The calculated mean stress exponent $n$=7.6782. The mean of the slopes in Fig. 6 was also calculated and it is 2.7145.

By substituting the mean values into Eq. 7, the $Q$ value can be calculated, and it is 173.2914 kJ/mol which higher than that of lattice self-diffusion in magnesium alloys [15].

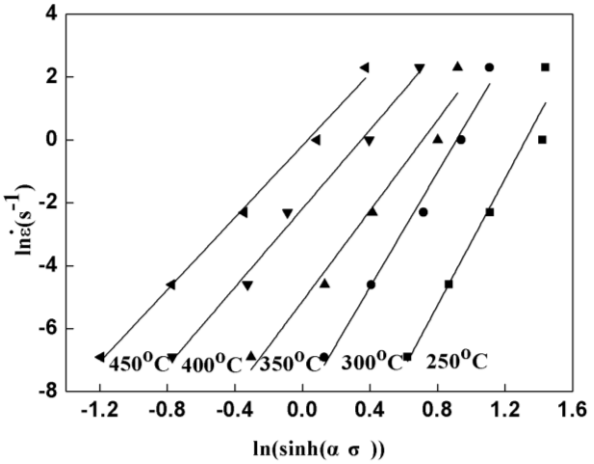


Fig. 5 Relationship between lnsinh(ln(ασ))-$\ln\dot{\varepsilon}$

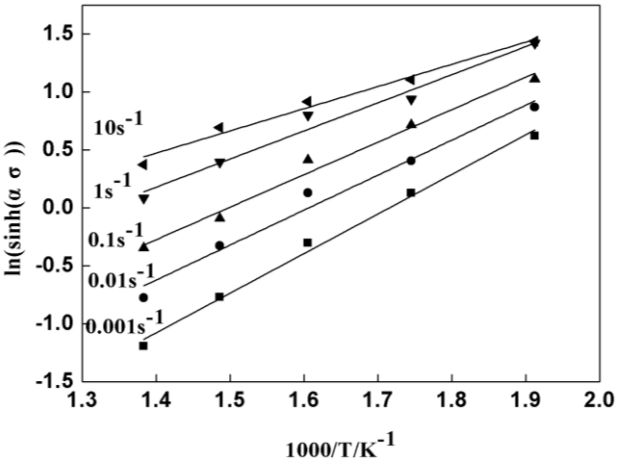


Fig. 6 Relationship between ln(sinh(ασ))-1000/T

Zener and Hollomon found that $Z$ parameter is depended on deformation temperature and the stain rate[18], They proposed that a materials flow stress could be described as a function of stain, stain rate, and temperature. The constitutive law can be expressed by a Zener-Hollomon parameter $Z$[19, 20].

$$Z = \dot{\varepsilon}\exp(\frac{Q}{RT}) = A[\sinh(\alpha\sigma)]^{n} = A'\sigma^{n} = A''\exp(\beta\sigma) \tag{8}$$

By logarithmic transformation of Eq. 8, the following expression is obtained:

$$\ln Z = \ln A + n\ln(\sinh(\alpha\sigma)) \tag{9}$$

The relationship between ln$Z$ and ln[sinh(ασ)] can be plotted as shown in Fig. 7. The values of $A$ and $n$ can be easily calculated as $4.64\times10^{12}$ and 7.336 from the data of Fig. 7, respectively. And the correlation coefficient is 0.96. Then the $Z$-parameter constitution equation for AE42 alloy can be described as:

$$\ln Z = 29.0158 + 7.336\ln(\sinh(\alpha\sigma)) \tag{10}$$

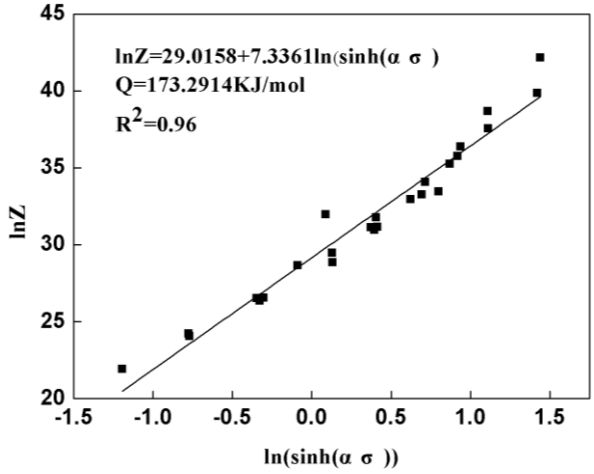


Fig. 7 plot of ln$Z$-ln(sinh(ασ))

The $\alpha$ is calculated using $n'$=11.4325 $MPa^{-1}$ and $\beta$= 0.1727 $MPa^{-1}$ as above mentioned, thus α =$\beta$/n'=0.0151. Finally, substituting the values of $\alpha$, $n$, $A$ and $Q$ into Eq. 3, the hyperbolic sine constitutive equation for AE42 magnesium alloy during high temperature compression is:

$$\dot{\varepsilon} = 4.64\times10^{12}[\sinh(0.0151\sigma)]^{7.336}\exp(-\frac{173291}{RT}) \tag{11}$$

To verify the three constitutive equations whether suitable for AE42 magnesium alloy or not, a comparison between the measured and predicted stress for three constitutive equations are carried out as shown in Fig. 8. It can be seen that the hyperbolic sine law constitutive equation is more suitable for AE42 magnesium because the predicted values and the measured values agree with very well. The correlation coefficients of the power law, the exponent law and the hyperbolic sine law constitutive equation are 0.87, 0.98, and 1, respectively. The results indicate that the proposed the hyperbolic sine law constitutive equation can be applied allover stress range for the AE42 magnesium alloy tested in this paper.

## Summary

The hot compression behavior of AE42 magnesium alloy was investigated by mean of isothermal compression in the temperature range of 250-450 ℃ and strain rate range of 0.001-10 s−1. The following conclusions have been drawn:

The flow stress-stain curves exhibit a peak stress in the initial stage of the deformation due to working hardening, and then stress reaches a steady stage due to equilibrium of working hardening and dynamic softening. The deformation temperature and stain rate affect the flow stress significantly. The flow stress increases with the strain rate increasing and/or the deformation temperature decreasing.

It is found that hyperbolic sine law is more suitable for AE42 magnesium alloy. The calculated stress exponent and activation energy are 7.34 and 173.29 kJ/mol, respectively. The activation energy of AE42 is slightly higher than that of lattice self-diffusion of pure magnesium. The constitutive equation for AE42 is:

$$\dot{\varepsilon} = 4.64\times10^{12}[\sinh(0.0151\sigma)]^{7.336}\exp(-\frac{173291}{RT})$$

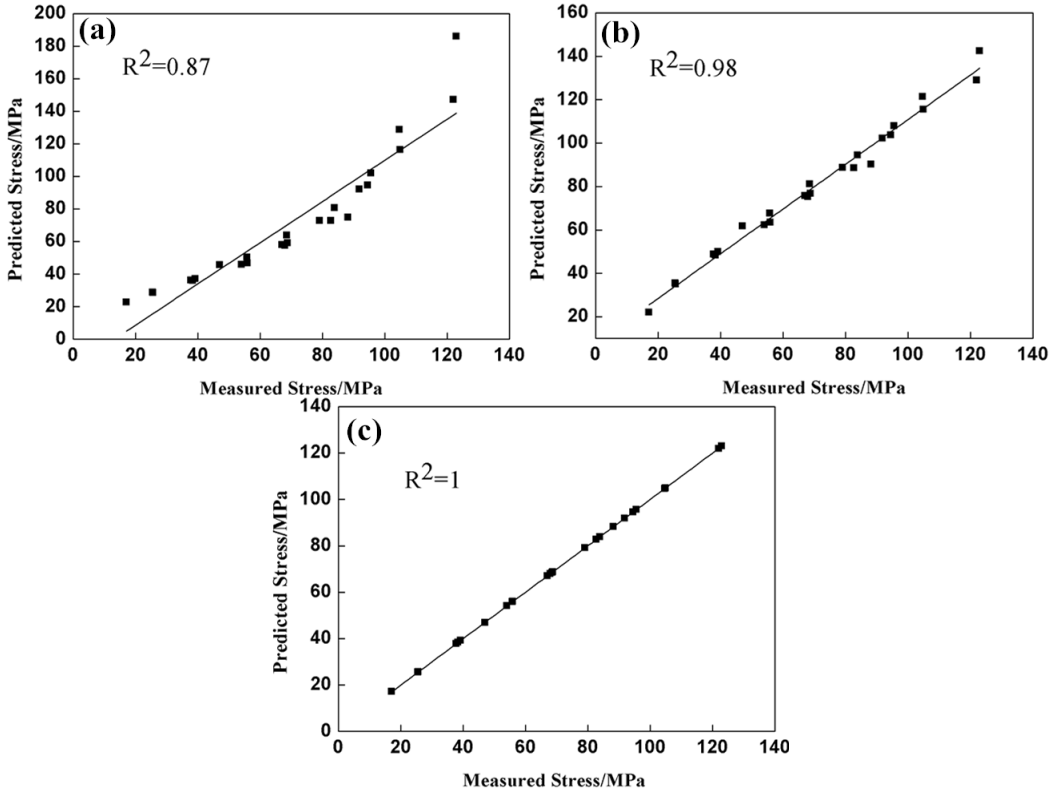


Fig. 8 comparison between predicted and measured σ values:(a)the power law (b)the exponent law, (c) the hyperbolic sine law


## Acknowledgment

This work was financially supported by the Foundation for Middle-aged and young of Qinghai University(No. 2014-QGY-11) and the Foundation for Middle-aged and young of Qinghai University(No. 2014-QGY-3).


## References


[1] C.Dharmendra, K.P.Rao, and F.Zhao, Effect of silicon content on hot working,processing maps and microstructural evolution of cast TX32–0.4Al magnesium alloy, Materials Science & Engineering A, 2014, 606: 11–23.

[2] T.Y.Kwak and W.J.Kim, Hot compression behavior of the 1wt% calcium containing Mg–8Al–0.5Zn(AZ80) alloy fabricated using electromagnetic casting technology, Materials Science & Engineering A, 2014, 615: 222–230.

[3] Robert.E, and Brown.B, Magnesium alloys and their applications international conference, Light Metal Age, 1998, 56.

[4] Jiang Xinyi, Xue Feng, and ZhaoKuo, Microstructures and mechanical properties of Mg-Al-RE alloys, Journal of southeast university(Natural Science Edition), 2010, 3(40): 676-651.

[5] J.Polme, Magnesium Alloys and applications, Materials Science and Technology, 1994, 10, l-16.

[6] Li Jones H, Eeffct of Rear Earth and Silicon Additions on Structure and Properties of Melt Spun Mg-9Al-1Zn Alloy, Materials Science and Technology, 1996, 12(8): 651-661

[7] Wei L Y, Dunlop G L, and Westengen H, Development of Microstructure in Cast Mg-Al-rare-earth Alloys, Materials Science and Technology, 1996, 12(9): 741-750.

[8] Mingliang Wang, Peipeng Jin, and Jinhui Wang, Hot Deformation and Processing Maps of 7005 Aluminum Alloy, High Temp. Mater. Proc. 2014; 33(4), 369 – 375.

[9] Mingliang Wang, Peipeng Jin, and Jinhui Wang, Hot Deformation Behavior and Workability of (SiCp+Mg2B2O5w)/6061Al Hybrid and SiCp/6061Al Composites, Acta Metall.Sin.(Engl. Lett.), 2014, 27(1): 63-74.

[10] S. Gall.M, Huppmann.H, and Mayer.S, Hot working behavior of AZ31 and ME21 magnesium alloys, J Mater Sci, 2013, 48: 473–480.

[11] Jing WANG, Bao-liang Yuan, and Sheng YANG, Hot compression behavior and processing map of cast Mg−4Al−2Sn−Y−Nd alloy, Trans. Nonferrous Met. Soc. China, 2014, 24: 626−631.

[12] Horng yu Wu, Cheng tao Wu, and Jie-chenYang, Hot workability analysis of AZ61 Mg alloys with processing maps, Materials Science & Engineering A, 2014, 607: 261–268.

[13] Yun peng Zhu, Peipeng Jin, and Peitang Zhao, Hot deformation behavior of Mg2B2O5 whiskers reinforced AZ31B magnesium composite fabricated by stir-casting, Materials Science & Engineering A ,2013, 573:148–153.

[14] Ming-liang WANG, Pei-peng JIN, and Jin-hui WANG, Hot deformation behavior of as-quenched 7005 aluminum alloy, Trans. Nonferrous Met. Soc. China, 2014, 24: 1−9.

[15] Bin Chen, Wei-Min Zhou, and Song Li, Hot Compression Deformation Behavior and Processing Maps of Mg-Gd-Y-Zr Alloy, Journal of Materials Engineering and Performance, 2013, 22: 2458–2466.

[16] H.J. McQueen and N.Ryan, Constitutive analysis in hot working, Materials Science and Engineering A, 2002, 322: 43–63.

[17] Xiang sheng Xia, Qiang Chen, and Jianping Li, Characterization of hot deformation behavior of as-extruded Mg–Gd–Y–Zn–Zr alloy, .Journal of Alloys and Compound ,610 (2014), 203–211.

[18] C. Zener and J. Hollomon, Effect of Strain Rate Upon Plastic Flow of Steel, J. Appl. Phys.,1944, 15: 22–32.

[19] M. Roostaei, M.H. Parsa, and R. Mahmudi, Hot compression behavior of GZ31 magnesium alloy, Journal of Alloys and Compounds, 2015, 631: 1–6.

[20] Hamed Mirzadeh, Constitutive analysis of Mg-Al-Zn magnesium alloys during hot deformation, Mechanics of Materials, 2014, 77: 80-85.